

Dynamics of vortex processes in thin-film bridge structures made of high T_c superconductors

K. I. Konstantinyan, G. A. Ovsyannikov, L. É. Amatuni, and Z. G. Ivanov¹⁾

Institute of Radiophysics and Electronics, Academy of Sciences of the Armenian SSR;

Institute of Radio Engineering and Electronics, Academy of Sciences of the USSR

(Submitted 21 September 1990)

Zh. Eksp. Teor. Fiz. **99**, 675–686 (February 1991)

Dynamic rf effects in bridge structures made of thin films of high T_c superconductors have been studied experimentally. The resistive state of such structures stems from the motion, driven by the Lorentz force, of magnetic flux quanta (vortices), whose shape in granular high T_c superconductors differs from that of Abrikosov or Josephson vortices. Experiments have been carried out on the narrow-band excitation of electromagnetic waves in bridge structures and on the locking of this excitation process by an external signal. The excitation and the locking are observed in the course of coherent motion of vortices under conditions of weak pinning. If the pinning is instead very strong, structural features are seen on the plot of the impedance of the structure versus the static electric field. The experimental results are compared with the predictions of existing theoretical models.

1. INTRODUCTION

In most cases, the high T_c superconductors may be thought of as granular Josephson media consisting of superconducting particles of size a_0 which are connected by Josephson junctions with a critical current I_c . The first theoretical work on a Josephson medium was reported in papers by Giovanini and Weiss,¹ Rosenblatt *et al.*,² and others in connection with the problem of granular superconductors. The theory of a Josephson medium has recently been expanded substantially by Clem³ and Sonin *et al.*⁴

Manifestations of coherence effects are seen. For example, current steps are seen on the current-voltage characteristic during the application of a microwave field to bridge structures made of high T_c superconductors with constriction sizes considerably larger than the coherence length ξ . Several authors explain these coherence effects on the basis that only one of the multitude of weak links between grains in the superconductor is actually "working." On the other hand, it has been demonstrated experimentally⁵⁻⁷ that effects characteristic of Josephson junctions can also arise in high T_c bridge structures from the coherent motion of magnetic flux quanta (vortices) driven by the transport current I and an external microwave field. These effects are quite familiar in the case of bridge structures made of homogeneous superconductors (In, Sn, etc.).⁸⁻¹⁰

A distinctive feature of bridge structures made of high T_c superconductors is that not only Abrikosov vortices but also vortices of two other types can arise and move. These two other types are Josephson vortices and hypervortices.⁴ Support for the argument that vortices move coherently in micron-size bridge structures comes from the experimental observation of a narrow-band emission in the microwave range.⁶ Despite the large number of studies which have been carried out on the electrical and magnetic properties of high T_c bridge structures, no data have been reported on the dynamics of vortex processes, aside from the results found in studying noiselike generation from millimeter-size bridge structures.¹¹

Our purpose in the present experimental study was to learn about dynamic rf effects (microwave generation, impedance, etc.) associated with vortex motion in high T_c

bridge structures under the influence of a transport current and an external magnetic field (of various intensities). We will compare our results with existing theoretical models.

2. THEORETICAL ASPECTS

Let us analyze the transport properties of a bridge structure which is fabricated from a superconducting film of thickness d by cutting the film in two places along a straight line running perpendicular to the transport current. The distance between the ends of the cuts determines the bridge width W , and the width of the cuts determines the length of the bridge structure, L . Aslamazov and Larkin have analyzed⁹ the electrostatics of such systems for a solid (i.e., not granular) film in the limit $L \rightarrow 0$ with $\xi < W < \lambda$, where λ is the magnetic-field penetration depth (this is the "Aslamazov-Larkin theory"). We will generalize this theory below to the case of a granular film, drawing on the results of Ref. 4.

In the London electrostatics of superconductors, the superconducting current j_s , the average phase of the order parameter, ϕ , and the vector potential \mathbf{A} are related by the following expression⁴ at distances much greater than a_0 :

$$j_s = (2e/\hbar)g(\nabla\phi - 2\pi\mathbf{A}/\Phi_0), \quad (1)$$

where

$$g^{-1} = 16\pi^3\lambda_L^2/\Phi_0^2 + (E_J a_0)^{-1},$$

λ_L is the London depth for the penetration of a magnetic field into a homogeneous superconductor, $E_J = \hbar j_c^2/2e$ is the energy per unit area of a Josephson link between grains, j_c^2 is the critical current density, and $\Phi_0 = hc/2e$ is the flux quantum. It is assumed here that the phase and magnitude of the order parameter remain constant within grains and that all changes in the phase occur at intergrain boundaries.

For a homogeneous thin film, with $d \ll \lambda_L$, we have

$$(2e/\hbar)g = I_0/\pi d,$$

where

$$I_0 = c\Phi_0 d/8\pi e\lambda_L^2$$

is the critical current, at which the Meissner state of the thin

film becomes unstable with respect to penetration by Abrikosov vortices with the electromagnetic radius¹⁰

$$\lambda = \lambda_{\perp} = \lambda_L \operatorname{ctgh}(d/2\lambda_L). \quad (2)$$

If there is a weak link between grains, with $I_0 > j_c^g a_0 d$, there is no general change in the nature of the processes, but the depth to which a weak magnetic field penetrates into the film (the vortex size) becomes⁴

$$\lambda = \begin{cases} \lambda_J, & a_0 \gg \lambda_J \gg \lambda_L, \\ \lambda_J, & \lambda_J \gg a_0 \gg \lambda_L, \\ \lambda_J(\lambda_L/a_0)^{1/2}, & \lambda_L \gg a_0, \quad \lambda_J \gg (a_0\lambda_L)^{1/2}. \end{cases} \quad (3)$$

In the last two cases in (3), the structure of the vortex is quite different from that of Abrikosov vortices in homogeneous superconductors. Because of the large electromagnetic radius, such vortices are called "hypervortices."⁴ These vortices do not have cores with a suppressed order parameter, and their dynamic properties are much the same as those of Josephson vortices. The critical field for the appearance of vortices, $H_{c1} = 4\pi^2/\Phi_0 \ln(\lambda/a)$, is weak (on the order of the geomagnetic field, 0.1 Oe).⁴ Since the expression for the superconducting current as a function of the phase gradient is the same as that for a film of a homogeneous superconductor, aside from the substitution $(2e/\hbar)g = I_0/\pi d$, we can use the results of the Aslamazov-Larkin theory to analyze the processes in a bridge structure made of a granular superconductor in the case $W < \lambda$. We can also make use of the results of Refs. 4 and 12–14. Let us look at the basic results which follow from this analysis.

1. The superconducting current is distributed nonuniformly in the bridge structure, even in the case $W < \lambda$. At currents $I > I_0 = \pi(2e/\hbar)dg$, a potential barrier at the edge of the film prevents the penetration of vortices. That barrier disappears at

$$I = I_c \approx \pi d g (2e/\hbar) (W/a_{ef})^{1/2}, \quad (4)$$

where a_{ef} is the effective size of the vortex core, which would be ξ for Abrikosov vortices or a_0 for a Josephson medium.

2. If there are no pinning centers, a vortex in the bridge structure moves in a viscous manner, under the influence of a force proportional to the local current density. The vortex formation time is proportional to ΔI ($\Delta I = I - I_c$) and is independent of the dimensions of the structure. The time scale of the viscous motion is $t_{\eta} = \pi\eta e W^2/4\hbar I_c \propto W^{3/2}$, where η is the viscosity coefficient.

3. At currents near I_c , the current-voltage characteristic of the bridge structure is determined by the time required to surmount the edge barrier, and the proportionality $V \propto \Delta I^{1/2}$ holds. As the current is raised, a plateau is observed at a voltage $V = V_0 = \hbar\pi/et_{\eta}$ on the characteristic of a short bridge structure ($L < \lambda_J$). This plateau corresponds to the motion of one vortex. Each subsequent increase in the number of vortices creates a peak in the differential resistance on the current-voltage characteristic at $V = NV_0$, where N is the number of vortices in the bridge structure. The characteristic is linear at $N \gg 1$, and then becomes parabolic: $V \propto V_0 I^2/I_c J_0$.

4. The results of the Aslamazov-Larkin theory, which we have discussed at a qualitative level here, are not altered by the slight spread in the properties of the weak links between grains, e.g., the spread in the critical currents. How-

ever, even if there are no pinning centers in the structure a spread in the properties will cause additional fluctuations in the system, and these fluctuations will disrupt the coherent motion of the vortices driven by the current. As was shown theoretically in Ref. 12, this effect imposes limits on the dimensions of the bridge structure:

$$L < \lambda_J (I/I_c)^2 (\lambda_J/d)^2 (a_0^2 Q^2/\lambda_J)^{-1}, \quad (5)$$

where Q is a measure of the scatter in the properties of the grains of the Josephson medium. Condition (5) can easily be satisfied in experiments on micron-size bridges.

5. If there are defects in the granular structure, the picture changes substantially, since the current density increases near a defect, causing local nucleation of vortices. Numerical calculations¹³ on a two-dimensional lattice of Josephson junctions have shown that the first row of moving vortices forms near a defect of this lattice, while subsequent rows appear beside the first and interact strongly with it, despite the substantial length of the bridge ($L \gg \lambda_J$).

6. An arbitrary distribution of several pinning centers will suppress coherent emission from a lattice of moving vortices in a bridge structure. However, the regular nature of the vortex motion persists. It is seen as structural features on the plot of the microwave impedance of the structure.¹⁴

3. TEST SAMPLES AND EXPERIMENTAL PROCEDURE

Bridge structures of two types were studied in these experiments. The structures were made of thin films of $\text{YBa}_2\text{Cu}_3\text{O}_x$ with various constriction dimensions W and L . In the structures of the first type (the samples of lots G and F), films $d \approx 300$ nm thick were grown on a hot (600–700 °C) MgO substrate by laser evaporation. The films grown in this manner were highly oriented, with a grain size $a_0 \approx 300$ nm (Ref. 15). The bridge configuration was created by photolithography and etching with argon ions. In the samples of the second type (the samples of lots A and J), the films had a thickness $d \approx 0.8$ μm and a grain size $a_0 \approx 1$ μm . These films were grown by dc magnetron sputtering on a sapphire substrate with a ZrO_2 sublayer.¹⁶

Table I shows the properties at $T = 4.2$ K of some of the samples which we studied. The geometric dimensions of the samples and the grain size in the films were measured with a scanning electron microscope. The critical current density $j_c = I_c/dW$ was found from the value of the critical current measured at a voltage $V < 5$ μV across the bridge structure. The transition temperature was found by extrapolating $j_c(T)$ to zero. The Josephson penetration depth λ_J was evaluated from the expression for a distributed sandwich Josephson junction:

$$\lambda_J = (c\Phi_0/8\pi^2 j_c t_{ef})^{1/2}, \quad (6)$$

where $t_{ef} = t + 2\lambda_L$ is the effective penetration depth for the magnetic field between two grains. The depth λ_L was assumed to be 0.2 μm for YBaCuO ; it was assumed to be much larger than the thickness of the medium between grains, $t \sim \xi = 0.5$ –2 nm.

The current-voltage characteristic and curves of dV/dI versus I and V were measured at various temperatures over the range $T = 4.2$ –100 K and at various power levels of the external microwave field, P_e , in the wavelength regions $\lambda \approx 3$ and $\lambda = 1.4$ cm. The sample was shielded from the external

TABLE I. Properties of the bridge structures studied in these experiments.

Sample	Width $W, \mu\text{m}$	Length $L, \mu\text{m}$	Transition temperature, T_c, K	Current density $j_c, \text{A/cm}^2$	Josephson penetration depth $\lambda_J, \mu\text{m}$
G7.2	5	10	81	$6 \cdot 10^6$	0,1
G3.1	2	10	71	$8 \cdot 10^4$	0,9
G3.2	3	14	71	$8 \cdot 10^4$	0,9
G3.3	7	12	71	$7 \cdot 10^4$	1,0
G4.3	6	20	92	$7 \cdot 10^6$	0,1
F3.1	9	10	60	$4 \cdot 10^4$	1,2
A1.1	50	120	70	$2 \cdot 10^3$	5,6
J1.1	45	110	35	60	17
J1.2	50	120	40	$2 \cdot 10^2$	32

magnetic field by an alloy of the Permalloy type. This shield reduced the geomagnetic field by at least an order of magnitude. A static external magnetic field $H \leq 10$ Oe was applied in the direction perpendicular to the plane of the film. For measurements of the power level of the signal which arose in the region $\lambda = 3$ cm at a bridge structure not exposed to an external microwave field, the sample was placed at a gap in a microstrip line. One end of this line terminated in a section with a length of $\lambda/4$; the other end was connected by coaxial cable to the input of a low-noise amplifier with an overall noise temperature $T_N = 800$ K and a bandwidth $\Delta F = 3$ GHz. The signal was then measured either by a power meter with a filter bandwidth $\Delta F = 25$ MHz or by a spectrum analyzer in a band $\Delta F = 1$ MHz.

In the wavelength region $\lambda = 1.4$ cm, the value of P at the bridge was measured with a tunable superheterodyne radiometric receiver with a fluctuational sensitivity $\delta T = 0.1$ K at a maximum reception bandwidth $\Delta F = 300$ MHz, with a time constant $\tau = 1$ s. Over the entire range of central frequencies used, $f = 18\text{--}22$ GHz, the reception bandwidth in the receiver could be reduced in discrete steps to $\Delta F = 10$ MHz. For these measurements, the substrates with the bridge structures were placed at the center of a flattened waveguide section with a cross section of 11×1 mm. This waveguide section had a shorting plunger, which was adjusted to achieve the best matching at frequencies $18\text{--}22$ GHz. One end of the bridge structure was short-circuited to the wall of the waveguide. The other end was connected by coaxial cable to a direct-amplification radiometric receiver tuned to a frequency $f = 1.7$ GHz, with a fluctuational sensitivity $\delta T = 0.02$ K, a reception band $\Delta F = 36$ MHz, and a time constant $\tau = 1$ s.

In studying the properties of bridges subjected to weak electromagnetic fields, we used a method of radiometric probing, in which a signal at $f = 22$ GHz with a power $P_e \approx 100$ fW was applied to the sample through a system of attenuators and a microwave decoupler. This signal did not perturb the current-voltage characteristic of the bridge structure. The level δP of the signal reflected from the sample was measured by one of the radiometric receivers for the corresponding range. Standard microwave sources were used as the sources of the external radiation.

4. EXPERIMENTAL RESULTS AND DISCUSSION

4.1. Critical current and current-voltage characteristic.

Figure 1 shows the temperature dependence of the normalized critical current, $I_c(T)/I_c(4.2 \text{ K})$, for several of the samples. Also shown there are various theoretical predic-

tions for various types of superconducting structures. The solid lines show the predictions of the Ambegaokar-Baratoff theory for tunnel junctions and of the Kulik-Omel'yanchuk theory for weak links with a direct (i.e., nontunneling) conductivity, for both the dirty case (KO-1) and the clean case (KO-2) (see the review by Likharev¹⁷). We find a reasonable agreement with both the KO-2 theory, which is valid for short weak links ($t/\xi < 1$, $l \gg t$, where l is the mean free path), and the theory for SNS junctions in the dirty limit (the dashed lines in Fig. 1) with a ratio $t/\xi = 2\text{--}3$.

Since the condition for a weak link between grains, which is basically a limitation on the critical current density $j_c < 2 \cdot 10^6$ A/cm², holds for all the bridge structures which we studied at $\lambda_L = 0.2 \mu\text{m}$ and $a_0 = 30$ nm, the only quantity in expression (4) for $I_c(T)$ which depends on the temperature is g , which is determined by the critical current between grains. The temperature dependence $I_c(T)$ which we measured (Fig. 1) thus reflects the temperature dependence of the intergrain critical current. The agreement of the experimental $I_c(T)$ curve with the KO-2 theory is evidence that the interlayers between grains in these films have a nontunneling conductivity and correspond to short weak links

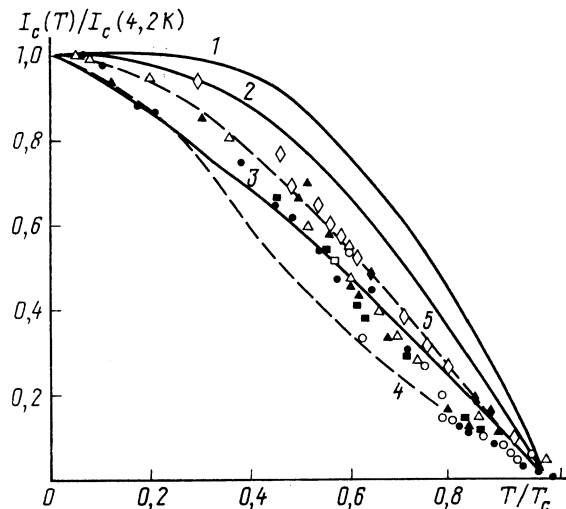


FIG. 1. Temperature dependence of the normalized critical current of several of the bridge structures which were studied. Solid lines: Theoretical predictions for (1) tunnel junctions (the Ambegaokar-Baratoff theory) and (2, 3) junctions with direct (i.e., nontunneling) conductivity of the interlayer (the Kulik-Omel'yanchuk theory), in the dirty limit (line 2; KO-1) and in the clean limit (line 3; KO-2). Dashed lines: Theoretical predictions for SNS junctions in the dirty limit for various values of the ratio t/ξ . 4— $t = 3\xi$; 5— 2ξ . \diamond —G 4.1; \circ —G 7.2; \bullet —G 3.3; \blacktriangle —F 3.1; \triangle —G 3.1; \blacksquare —G 3.2.

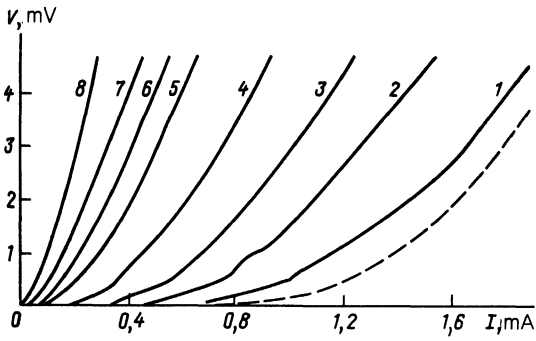


FIG. 2. Family of current-voltage characteristics of bridge structure *G* 3.2 at various temperatures: 1—4.2; 2—31; 3—36; 4—44; 5—49; 6—53; 7—57; 8—59 K. The dashed line is the characteristic of structure *G* 7.2 at $T = 16.4$ K, plotted in a different scale ($I/3, 5V$).

in the clean limit, rather than to *SNS* junctions, because of the small value $\xi \sim t < l$ (Ref. 18). The nonlinear dependence $I_c \propto (T_{c0} - T_c)^n$ ($n = 1.5-2$) near T_c is probably due to suppression of phase coherence in the Josephson medium by temperature fluctuations ($kT \sim Ej$). This behavior of I_c near T_c is seen most clearly in the bridge structures with low current densities, because fluctuations have a stronger effect in that case.

Figure 2 shows current-voltage characteristics of bridge structure *G* 3.2 at various temperatures. There is no hysteresis on these characteristics over a wide temperature range. The presence of an excess current on the characteristics (i.e., a shift of the characteristics with respect to an ohmic asymptote at high voltages), which is typical of weak links with a direct conductivity, supports our suggestion that the properties of this bridge structure are those of a system of grains coupled by weak links with a direct conductivity. The current-voltage characteristic of a bridge structure at a low temperature consists of several regions in which the differential resistance R_d remains essentially constant, separated by some unstable regions in which the value of R_d changes.

For this particular structure the relation $\lambda_J > a_0 \approx \lambda_L$ holds over a wide temperature range (4–50 K), and the depth to which a magnetic field penetrates into the superconductor (the size of the hypervortex) is λ_J , according to (3). In this case, irregularities of the structure itself (with a size on the order of a_0) have only a weak effect on the motion of vortices. As a result, the vortices move in a viscous fashion, with a force proportional to the local current density, and regions with a constant differential resistance $R_d = R_0$ form on the current-voltage characteristic.

From Ref. 4 we have $R_0 \propto n_v/\eta$, where n_v is the density of vortices in the bridge structure. In our experiments we observe $R_0 \propto I_c(T)^{-1/2}$ as the temperature is varied. This behavior agrees with the Aslamazov-Larkin theory for the case $H = 0$, $n_v = \text{const}$, $I > I_c$, if we assume $\eta \propto \lambda_J^{-1}$, as for Josephson vortices. Because of the large length of this bridge, $L \gg \lambda_J$, the number of rows of vortices in the bridge increases with increasing current. This is the case which is most commonly seen experimentally, but it is not covered by the Aslamazov-Larkin theory. As the current is raised, the first row is joined by other rows, at a distance comparable to λ_J . As a result, the values of R_d in the linear regions on the current-voltage characteristic increase in a discrete fashion;

again, this is what is observed experimentally. At $I > I_c$, the number of vortices in the bridge, N , and their velocity v increase $\propto I$. As a result, the current-voltage characteristic is parabolic ($V \propto I^2$), again in agreement with the Aslamazov-Larkin theory.

The unstable regions on the current-voltage characteristic, with a negative R_d , are probably the result of thermally activated flux creep.⁶ In bridges with size $\lambda_J < a_0$ or in bridges made of a greatly disordered film (with irregularities at distances on the order of λ_J), the viscous motion of the vortices is disrupted by the pronounced pinning. Structure *G* 7.2, for example, has a high j_c , a low $\lambda_J \approx 0.1 \mu\text{m}$, and $a_0 \approx 0.3 \mu\text{m}$, and there are no regions with a constant R_d on the current-voltage characteristic (see the dashed line in Fig. 2). In this case, the dominant process in the resistive region of the current-voltage characteristic is thermally activated creep of magnetic flux.

4.2. Electromagnetic radiation. Figure 3 shows current-voltage characteristics of a bridge structure and the voltage dependence of the power radiated by this structure, $P(V)$, for the case in which no microwave field is applied to the bridge. Electromagnetic radiation is observed to be emitted as several peaks at voltages up to 0.5 mV. This $P(V)$ behavior is quite different from that which is observed in Josephson bridges made of homogeneous superconductors.¹⁹ The voltage corresponding to the appearance of the first emission peak is related to the emission frequency f_e by

$$V_{m,n} = (n/m) h f_e / 2e, \quad (7)$$

where n and m are integers ($m = 1$ and $n = 1$ for this particular peak). This result and also the approximately linear region on the current-voltage characteristic with $R_d = R_0 = \text{const}$ at V up to $\sim 200 \mu\text{V}$ are evidence that there is one row of vortices in the bridge. At a given current through the bridge, the motion of the vortices is periodic. As each vortex passes, it causes a change of 2π in the difference between the quantum-mechanical phases of the superconducting banks of the bridge. As a result, each vortex induces an alternating component of the voltage with a frequency

$$f = Nv/b, \quad (8)$$

where b is a characteristic size of the vortex lattice ($b \sim W$).^{9,10}

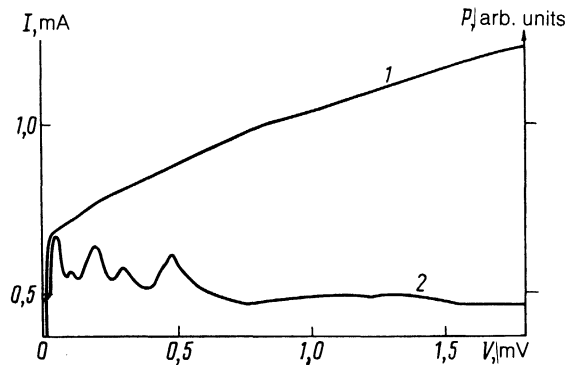


FIG. 3. 1—Current-voltage characteristic in the case without an external microwave field; 2—voltage dependence of the power of the intrinsic emission of bridge *G* 3.2 at a frequency $f = 7.896$ GHz ($\Delta F = 25$ MHz, $T = 4.2$ K).

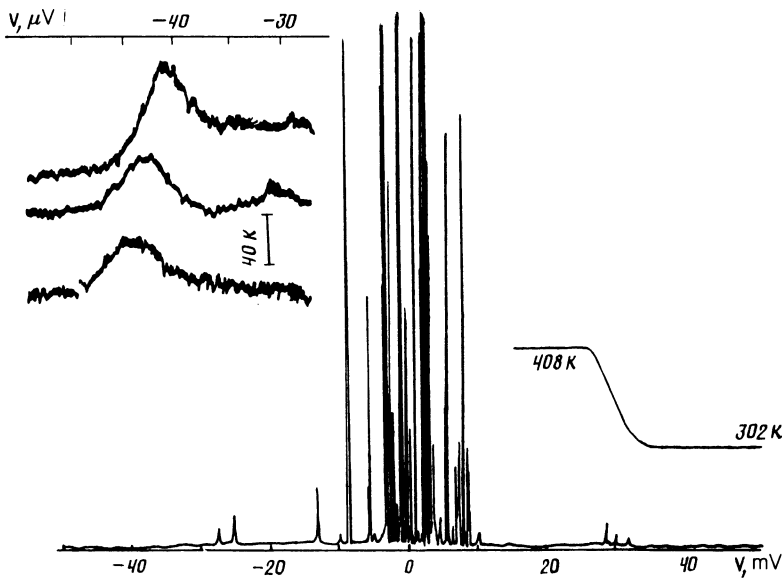


FIG. 4. Power emitted by bridge *A* 1.1 at the frequency $f = 21.15$ GHz at $T = 4.2$ K. Shown at the right is a calibration step, from the temperature drop of matched loads placed at the receiver input. The inset shows $P(V)$ for an end-type Nb-Si-Nb Josephson junction¹⁹ at $T = 4.2$ K at three frequencies: $f = 17.9, 19.3,$ and 21.8 GHz.

At high voltages ($V > V_{1,1}$), the emission spectrum $P(V)$ of the bridge has unequally spaced peaks. The new peaks on the $P(V)$ curve appear (as V is increased) on a part of the current-voltage characteristic with a large value of R_d . This result corresponds to the presence of several vortex rows in the bridge. On occasion, one observes several peaks on a part of the characteristic with $R_d = \text{const}$, apparently because changes occur in both $N(I)$ and $v(I)$, but the product Nv remains constant [see (8)]. Subsequent rows of vortices appear in a bridge with $L \gg \lambda_j$ in the immediate vicinity of the first row and interact strongly with it, according to Ref. 13. As can be seen from the experimental results (Figs. 3 and 4), however, no significant increase in the radiated power is observed as the number of vortex rows increases, with the corresponding change in R_d of the bridge. The probable explanation here is that the excitation process in neighboring rows are out of phase. As a result, as the number of vortex rows increases, the value of P does not exceed the power level corresponding to the motion of a single row.

We found similar results for a second lot of bridges, *A* 1.1, with relatively large dimensions and relatively low current densities ($\lambda_j \approx 5.6 \mu\text{m}$; Fig. 4). In this case the microwave emission at 21 GHz was observed at voltages up to $V_{\text{max}} \approx 8$ mV. The ratio $V_{\text{max}}/V_{1,1} > 180$ corresponds to filling of the entire area of the bridge by moving vortices, $WL/\lambda_j^2 \approx 190$, if it is assumed that each successive emission peak is caused by an increase in the number of vortices in the bridge. We observed the same results for the bridges of lot *G*. When a static magnetic field $H < 10$ Oe was imposed on the bridge, the amplitude of the emission increased by a factor of 5–7.

A spectrum analyzer was used to measure the width of the emission line for bridge *G* 3.2 in a weak magnetic field. The result was²⁾ $\Delta f \approx 300$ MHz. This is only twice the width of the emission line corresponding to a single Josephson junction with the same value of R_N . The maximum value of the emission power of bridge *A* 1.1 at $f \approx 21$ GHz was estimated; allowance was made for the impedance mismatch of the bridge and the microwave line and for the loss in the microwave line. The result is $P \approx 3 \cdot 10^{-11}$ W. This figure is much higher than the value which has been found experimental-

ly¹⁹ for Josephson bridge junctions and also much higher than the value of P measured in our electrodynamic system when the high T_c superconducting bridge was replaced by an end-type Josephson junction²⁰ (see the inset in Fig. 4).

4.3. *Effect of an external microwave field.* Figure 5 shows current-voltage characteristics and a plot of $P(I)$ for bridge *A* 1.1 when it is not in a microwave field and also when a microwave signal is applied at a frequency outside the reception band. The shape of the current step which forms on the current-voltage characteristic at $V_{1,1}$ is hyperbolic, in agreement with the predictions of the Aslamazov-Larkin theory. The shape of the $P(I)$ curve near the current step is precisely the same as that for a Josephson junction.

Figure 6a shows a family of $P(V)$ curves at $f = 1.7$ GHz for various power levels of the external microwave field, with $f_e = 21$ GHz, for bridge *J* 1.1, with a large normal resistance, $R_N = 220 \Omega$, and $I_c = 30 \mu\text{A}$ (a small value of j_c). The slight intrinsic emission at $V \approx 3$ and 14 mV is seen to depend on the external electromagnetic field P_e . Figure 6b

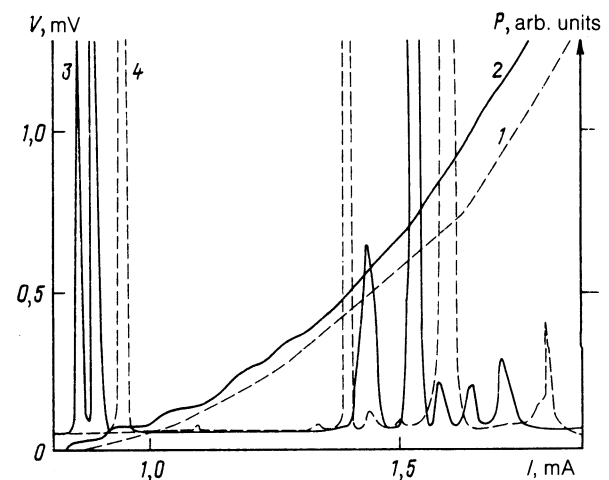


FIG. 5. 1, 2—Current-voltage characteristics; 3, 4—current dependence of the emission power. Dashed lines) In the case in which no microwave field is applied; solid lines) when an external microwave field is applied with a frequency outside the reception band, $f_c = 21$ GHz.

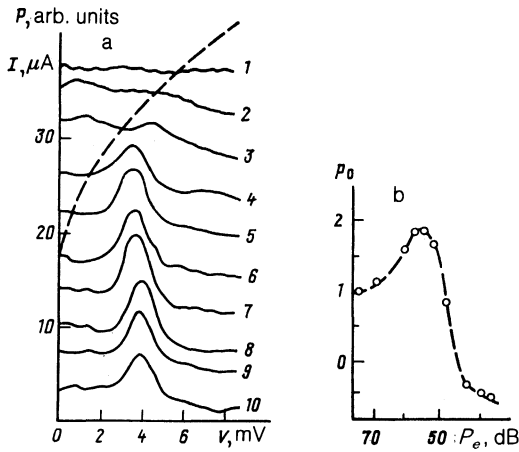


FIG. 6. a: Family of curves of the power $P(V)$ of the intrinsic emission of bridge structure $J1.1$ at $f \approx 1.7$ GHz for various power levels of the external microwave field at $f_e \approx 21$ GHz, at $T = 4.2$ K, and for various values of the attenuation in the microwave line. 1— $P_e = 35$; 2—40; 3—42; 4—48; 5—52; 6—55; 7—57; 8—60; 9—70; 10— ∞ dB. The dashed line is the current-voltage characteristic. b: The normalized power $p_0 = P(V \approx 3 \text{ mV})/P(V = 0)$ versus P_e . The level $P(V = 0)$ corresponds to the power level of the background radiation for $I < I_c$.

shows the experimental results on the normalized emission power $p_0 = P(V \approx 3 \text{ mV})/P(V = 0)$ as a function of P_e . We see that for values of P_e corresponding to values $\alpha \approx 70$ –45 dB of the attenuation by the attenuator the emission power is higher than that for a bridge to which no microwave field is applied. This $p_0(P_e)$ behavior probably occurs because a weak external agent with a microwave current $I_- < I_c$ causes ordering of the motion of the vortices, and this ordering stimulates the intrinsic emission. Over the entire P_e range shown in Fig. 6, the current-voltage characteristic remains unperturbed (the change in I_c is less than 5%). Possible frequency-conversion effects are negligible since there is no intrinsic emission near the frequency f_e at low power levels of the incident signal ($P_e < 0.1$ nW).

Figure 7 shows a current-voltage characteristic and a plot of the microwave signal reflected from the bridge, $\delta P(I)$, recorded at $f \approx 22$ GHz at $T = 4.2$ K for bridge $J1.2$ with $R_N = 180 \Omega$. We see that the shape of the $\delta P(I)$ curve is definitely not monotonic. There are several plateaus, which correspond to certain intervals of ΔI of the transport current in which the impedance of the bridge remains constant. According to Ref. 14, the motion of the vortex rows remains

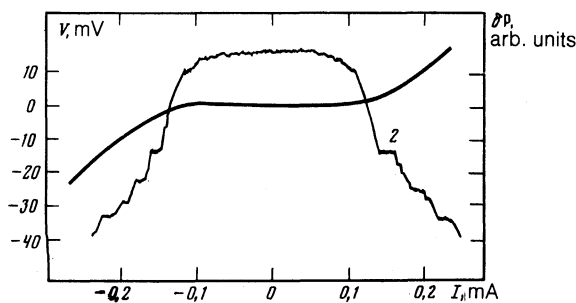


FIG. 7. 1—Current-voltage characteristic; 2—current dependence of the signal reflected from bridge $J1.2$, $\delta P(I)$. These results were obtained at $T = 4.2$ K at a power level $P_e \approx 10^{-13}$ W and a frequency $f_e \approx 21$ GHz of the external microwave field.

regular in a superconducting film with randomly distributed pinning centers, even if there is no intrinsic emission in the bridge. The interaction of a moving lattice of vortices with an external electromagnetic field gives rise to structural features on the I dependence of the quantity δP , which is proportional to the impedance $Z(E)$ of the high T_c bridge (E is the static electric field), at values

$$E_{p,q} \approx (p/q) f_e (\Phi_0 H/c)^{1/2} \quad (9)$$

of the static electric field, where H is the magnetic field, and p and q are integers. Analysis of the data in Fig. 7 yields the voltage interval between jumps in $Z(V)$ for $p = \pm 1$, $q = \pm 1$ and for $p = \pm 2$, $q = \pm 1$: $\Delta U = V_{\pm 2, \pm 1} - V_{\pm 1, \pm 1} \approx 3 \text{ mV}$. For $f_e \approx 21$ GHz, these results correspond to an estimate $H \approx 0.05$ Oe, according to (9), of the residual field at the sample in the shield of the alloy of the Permalloy type. The jumps in the impedance at $\Delta U/2$ and $\Delta U/3$ correspond to harmonics of the external agent, $2f_e$ and $3f_e$. We did not observe subharmonic structural features with $q > 1$. The asymmetry of the $\delta P(I)$ curve with respect to $I = 0$ is characteristic of vortex processes in high T_c superconductors. It has been seen previously for the current-voltage characteristics of bridges.⁵

5. CONCLUSION

The results of these experiments on dynamic effects in bridge structures made of high T_c superconductors demonstrate the following:

1. The film structures made of $\text{YBa}_2\text{Cu}_3\text{O}_{7-x}$ studied in these experiments may be regarded, at least at low current densities ($j_c < 10^6 \text{ A/cm}^2$), as consisting of a granular Josephson medium of grains with a nontunneling conductivity of the links between grains. These links may be described as contacts between superconductors in the clean limit.

2. The electrical and microwave properties of micron-size bridges of these films can be explained in terms of processes involving the motion of vortices driven by the transport current and the microwave field, even in the absence of an external magnetic field.

3. When the irregularities in the films of the bridge structures with dimensions $W, L \sim \lambda_J$ are small, viscous motion of vortices is driven by the transport current. This motion is manifested by the appearance of coherence effects such as Shapiro steps and intrinsic emission of electromagnetic waves.

4. During the coherent motion of vortices in a bridge, one observes emission with a linewidth close to that predicted for a Josephson junction. The maximum detected emission power was $3 \cdot 10^{-11} \text{ W}$.

5. Pinning centers, if present, prevent coherent motion of vortices, but they do not disrupt the regular nature of the motion of the vortices. An external microwave field can raise the degree of order of the vortex motion. The effect is manifested experimentally by an increase in the intensity of the intrinsic emission and also nonmonotonic behavior of the microwave impedance of the bridge as a function of the static electric field.

We wish to thank T. Claeson for a useful discussion and for critical comments during the part of this study which was carried out at Chalmers Technological University in Sweden. We also thank J. Alarko for measurements with the

electron microscope; G. Brorsson, D. G. Emel'yanenkov, V. N. Laptev, and V. I. Makhov for fabricating the samples; A. A. Akhmyan, J. Bindslev-Hansen, and A. Ustinov for valuable discussions; and R. M. Martirosyan for constant interest in this work. This work was supported by the Scientific Council on the Problem of High Temperature Superconductivity and was carried out within the framework of Projects 42 and 2068 of the State "High Temperature Superconductivity" Program.

¹⁾ Institute of Electronics, Bulgarian Academy of Sciences, Sofia.

²⁾ In a recent paper published at the same time as our own,¹⁵ Jung *et al.*²¹ reported measurements of the width of the emission line at a lower frequency. Their result, $\Delta f = 22$ MHz, is an order of magnitude smaller than our own.

¹ B. Giovanini and L. Weiss, *Solid State Commun.* **27**, 1005 (1978).

² J. Rosenblatt, *Rev. Phys. Appl.* **9**, 217 (1974).

³ J. R. Clem, *Physica C* **153-155**, 50 (1988).

⁴ E. B. Sonin, *Pis'ma Zh. Eksp. Teor. Fiz.* **47**, 415 (1988) [*JETP Lett.* **47**, 496 (1988)]; E. B. Sonin and A. K. Tagantsev, *Zh. Eksp. Teor. Fiz.* **95**, 994 (1989) [*Sov. Phys. JETP* **68**, 572 (1989)].

⁵ L. E. Amatuni, A. A. Akhmyan, K. I. Konstantinyan *et al.*, *Pis'ma Zh. Eksp. Teor. Fiz.* **49**, 559 (1989) [*JETP Lett.* **49**, 647 (1989)].

⁶ L. E. Amatuni, A. A. Akhmyan, R. B. Airapetyan *et al.*, *Pis'ma Zh.*

Eksp. Teor. Fiz. **50**, 355 (1989) [*JETP Lett.* **50**, 385 (1989)].

⁷ M. A. M. Gijs, D. Terpstra, and H. Rogalla, *Solid State Commun.* **71**, 1881 (1989).

⁸ V. N. Gubankov, V. P. Koshelets, K. K. Likharev, and G. A. Ovsyannikov, *Pis'ma Zh. Eksp. Teor. Fiz.* **18**, 292 (1973) [*JETP Lett.* **18**, 171 (1973)].

⁹ G. L. Aslamazov and A. I. Larkin, *Zh. Eksp. Teor. Fiz.* **68**, 766 (1975) [*Sov. Phys. JETP* **41**, 381 (1975)].

¹⁰ K. K. Likharev, *Zh. Eksp. Teor. Fiz.* **61**, 1700 (1971) [*Sov. Phys. JETP* **34**, 906 (1972)].

¹¹ J. Konopka and G. Jung, *Europhys. Lett.* **8**, 549 (1989).

¹² A. F. Volkov, *Pis'ma Zh. Eksp. Teor. Fiz.* **49**, 86 (1989) [*JETP Lett.* **49**, 103 (1989)].

¹³ W. Xia and P. L. Leath, *Phys. Rev. Lett.* **63**, 1428 (1989).

¹⁴ A. T. Fiory, *Phys. Rev. B* **7**, 1881 (1973).

¹⁵ G. A. Ovsyannikov, Z. G. Ivanov, G. Brorsson, and T. Claeson, *Physica B* **165-166**, 1609 (1990).

¹⁶ D. G. Emel'yanenkov, Yu. I. Inkin, V. A. Kulikov *et al.*, *Pis'ma Zh. Tekh. Fiz.* **15**(11), 40 (1989) [*JETP Lett.* **15**(11), 847 (1989)].

¹⁷ K. K. Likharev, *Usp. Fiz. Nauk* **127**, 185 (1979).

¹⁸ L. P. Gor'kov and N. B. Kopnin, *Usp. Fiz. Nauk* **156**, 117 (1988) [*Sov. Phys. Usp.* **31**, 850 (1988)].

¹⁹ V. N. Gubankov, V. P. Koshelets, and G. A. Ovsyannikov, *Pis'ma Zh. Eksp. Teor. Fiz.* **21**, 489 (1975) [*JETP Lett.* **21**, 226 (1975)].

²⁰ A. L. Gudkov, K. K. Likharev, and V. I. Makhov, *Pis'ma Zh. Tekh. Fiz.* **11**, 1423 (1985) [*Sov. Tech. Phys. Lett.* **11**, 587 (1985)].

²¹ G. Jung, J. Konopka, and S. Vitale, *Physica* **165-166**, 105 (1990).

Translated by D. Parsons